Fluid−Liquid and Fluid−Solid Phase Behavior of Poly(ethylene-*co*-hexene-1) Solutions in Sub- and Supercritical Propane, Ethylene, and Ethylene + Hexene-1

Alan Ka Chun Chan and Maciej Radosz*

Department of Chemical Engineering and Macromolecular Studies Group, Louisiana State University, Baton Rouge, Louisiana 70803-7303

Received November 30, 1999

ABSTRACT: Fluid−liquid (FL) pressure and fluid−solid (FS) temperature of poly(ethylene-*co*-hexene-1) (EH) in sub- and supercritical propane and ethylene + hexene-1 mixtures are measured with a variable-volume batch optical cell. The effects of the EH concentration, weight-averaged molecular weight (M_w), branch density (BD), crystallizability, solvent type, and solvent ratio on the phase behavior are investigated at temperatures up to 180 °C and at pressures up to 1400 bar. Both EH concentration and M_w are found to have a relatively weak effect on the phase behavior. The FL pressure and FS temperature are found to decrease as BD increases. The FL pressure is also found to depend strongly on the solvent type. When the ethylene concentration increases in EH + ethylene + hexene-1 mixtures, the FL pressure is found to increase, whereas the FS temperature is found to decrease.

Introduction

The crucial challenge in processing polymeric materials from solution is how to separate the solvent. The subcritical liquid solvents are separated from polymer either by evaporation at low pressures or by dilution with an antisolvent. The supercritical solvents, on the other hand, can be separated by rapid expansion. Such a rapid-expansion separation is much faster and allows for a higher degree of flexibility in controlling the material morphology, for example, the shape and size of particles and pores. This rapid-expansion separation is applicable to supercritical-fluid and polymer pairs that exhibit complete miscibility. The pairs that do not exhibit a complete miscibility can be processed according to a hybrid approach: we dissolve the polymer in a subcritical liquid solvent, but then, instead of evaporating the solvent, we pressurize the solution with a supercritical antisolvent to form the solid material.

In all these approaches, the final material morphology sensitively depends on the phase-diagram path and the rates of changing the pressure, temperature, and composition, from the initial solution to the solvent-free material. It is the choice and optimization of this path that is the key to achieving a material of desired properties in a reproducible fashion. This, in turn, calls for understanding the solution phase behavior at high pressures.

A phase behavior example of a high-pressure polymer−solution system selected for this study is a linear polyolefin of variable crystallizability, poly(ethylene-*co*-hexene-1), EH for short, in three types of solvents: propane, an example of a sub- or supercritical solvent candidate for rapid-expansion processing, hexene-1, an example of a subcritical liquid monomer or solvent for conventional evaporation processing, and ethylene, an example of supercritical-antisolvent component in mixed solvents, for example, with hexene-1.

* Corresponding author's current address: Department of Chemical and Petroleum Engineering, University of Wyoming, Laramie, WY 82071-3295. E-mail radosz@uwyo.edu; tel 307-766-2500, fax 307-766-6777.

The phase behavior of polyolefin + alkane or polyolefin + olefin systems has been a subject of previous studies.[1−8] The emphasis of those previous studies was mostly on the fluid−liquid (FL) phase transitions. It turns out that, to develop a complete phase behavior picture, we also need semiquantitative data, models, and phase diagrams including the fluid−solid (FS) phase transitions.

The goal of this work, therefore, is to generate experimental data and to develop first-pass correlations for the FL and FS transitions in EH solutions in propane, ethylene, hexene-1, and ethylene + hexene-1. This is a preliminary study aimed at semiquantitative models that can account for the polymer crystallizability and molecular weight and for the solvent type and composition.

Generic Phase Diagrams

To understand the phase behavior of poly(ethylene-*co*-hexene-1) solutions in sub- and supercritical fluids, simple two-dimensional phase diagrams are usually helpful. Figure 1 shows two generic pressure−temperature phase diagrams: one for a monodisperse amorphous polymer−solvent system and one for a crystalline polymer−solvent system. In the case of the amorphous polymer system, if the differences in molecular weight and density between the polymer and solvent are small, a pair of FL phase boundaries exists: the lower critical solution temperature (LCST) boundary and the upper critical solution temperature (UCST) boundary. As the degree of the molecular asymmetry between the polymer and solvent increases (as pointed by the arrow), however, the LCST and UCST curves approach each other and eventually merge to form a single curve, the upper−lower critical solution temperature (U-LCST)[1] curve.

In the case of the crystallizable polymer system shown at the bottom of Figure 1, the phase behavior is more complex. LCST and UCST curves still exist, but the UCST curve or branch can be superseded by a FS boundary; the FS boundary merges then with the LCST boundary.

10.1021/ma991994k CCC: $19.00
Published on Web 08/03/2000

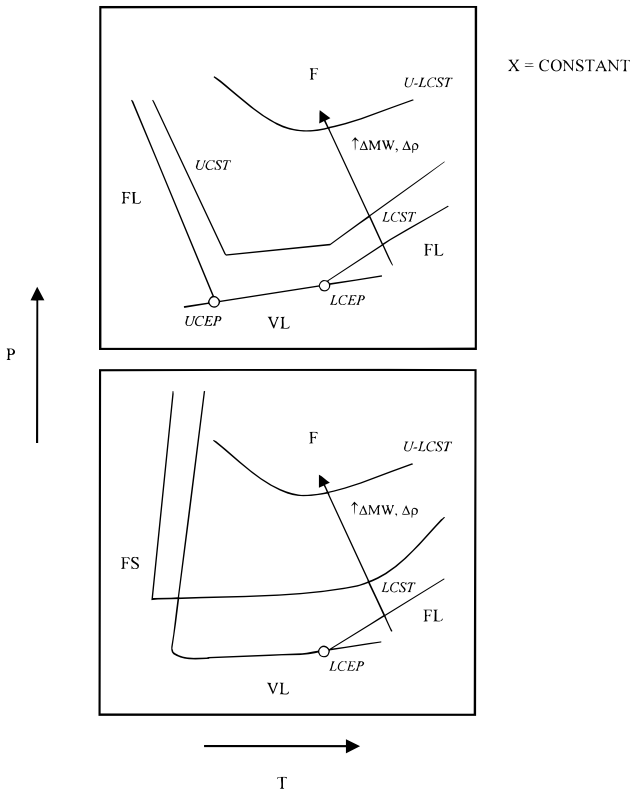

Figure 1. Generic $P-T$ phase diagram for an amorphous (top) and crystalline (bottom) polymer solutions.

Experimental Section

The FL and FS phase equilibria are measured in a variable-volume batch optical cell equipped with a transmitted-light probe. The layout, apparatus, and experimental procedure are described in detail elsewhere,[9] so only a brief overview is given here. The phase transitions can be either observed visually on a video monitor, via a borescope, or detected using a transmitted-light probe. The accuracy for the pressure transducer is ±0.5 bar and is ±0.1 °C for the temperature probe. A known amount of polymer and solvent is placed in the cell and well mixed until equilibrium is reached. The FL pressure, also referred to as the cloud-point pressure, is measured at constant temperature, and the FS temperature is measured at constant pressure. The cloud-point pressure is also characterized visually as being either of the bubble- or dew-point type.[9]

The FL pressure is measured by lowering the pressure until the mixture turns cloudy, which sharply decreases the transmitted-light intensity. The result is then checked by raising the pressure until the mixture is completely clear. The difference is found to be insignificant (less than 2 bar). Therefore, the pressure at which the mixture turns cloudy is taken as the FL pressure in this study. The FS temperature is measured isobarically by both cooling and heating; during cooling, the solution turns cloudy, and during heating, the cloudy solution turns clear. Both the cooling and heating rates are kept less than 1 °C min^{-1} to minimize kinetic effects. The difference between the cooling- and heating-induced FS temperature is found to be around 10−15 K. This is expected as suggested, for example, by Kohn et al.[10] and Condo et al.[11] The reason for this discrepancy between the cooling-induced and heating-induced FS temperature is a subcooling effect, which inhibits the nucleation of crystals in solution. The superheating effect, which inhibits the dissolution of crystals, is believed to be usually less significant, and hence, the heating-induced FS temperature is usually accepted as being closer to a true equilibrium FS temperature.

Materials. Four EH samples are used in this work. They all have a generic structure shown in Figure 2; the number of side butyl branches (shaded segments) per unit backbone

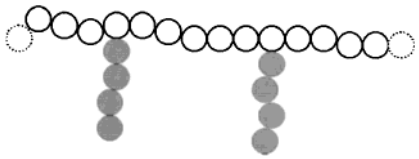

Figure 2. Generic EH structure.

Table 1. Properties of Polymer Samples

polymer sample	wt % hexene	BD	M_w/ kg mol^{-1}	M_w/M_n	DSC T_h/°C[b]	DSC T_c/°C[b]
EH-0-120K[a]	0	0	120	1.19	134.1	119.0
EH-4-80K	10.6	4	80	1.52	106.1	90.9
EH-15-100K	35.0	15	103	2.14		
EH-15-140K	35.0	15	139	1.24	40.6	24.3

[a] EH-0-120K = NIST SRM1484. [b] T_h = heating-induced temperature, T_c = cooling-induced temperature.

(blank segments) varies from sample to sample. These samples are characterized with differential scanning calorimeter (DSC), temperature rising elution fractionation (TREF), and gel permeation chromatography (GPC). Their properties are given in Table 1. These samples have polydispersity index around 2 or less. They are coded in terms of the branch density (BD) and the weight-averaged molecular weight (M_w); the first number in the sample code is BD, and the second number is M_w. BD is defined as the number of branches per 100 ethyl units in the polymer backbone, and hence it is a measure of the comonomer incorporation. The sample coded EH-0-120K is used in this study as a branch-free, limiting case for EH. It is a linear polyethylene fraction with a narrow molecular weight distribution purchased from the National Institute of Standards and Technology (NIST), designated as the Standard Reference Material (SRM) of 1484. EH-4-80K is a cross-fractionated sample: first fractionated with respect to crystallizability using preparative TREF in propane and then refractionated with respect to molecular weight using a pressure-increasing mode in supercritical propane. EH-15-140K is fractionated only with respect to molecular weight in supercritical propane, and EH-15-100K is used without fractionation or purification.

Ethylene (polymer grade, 99.9% minimum purity), purchased from Matheson Gas Products, propane (instrument grade, 99.5% minimum purity), purchased from Praxair, and hexene-1 (99+% purity), purchased from Sigma Chemical, are also used without further purification. To prevent the ethylene polymerization during the experiment, a small amount of butylated hydroxytoluene is added as an oxidation inhibitor as suggested by Spahl and Luft.[12]

Equation-of-State Correlation

The experimental data obtained in this work are correlated with two versions of the SAFT equation of state: SAFT[13,14] and SAFT1.[15] SAFT is developed on the basis of an argon equation of state for the segment term and a hard-sphere pair-correlation function for the chain term[13] and extended to heterosegmented molecules, such as copolymers.[14] SAFT1 is developed on the basis of a perturbation theory of square-well fluids (Barker−Henderson's perturbation theory) for the segment term and a square-well pair-correlation function for the chain term.[15]

The dimensionless residual Helmholtz energy of chain molecules $\tilde{a}^{res}$ in the SAFT equation of state can be expressed as

$$\tilde{a}^{res} = \tilde{a}^{seg} + \tilde{a}^{chain} + \tilde{a}^{assoc} \quad (1)$$

where $\tilde{a}^{seg}$ is the segment term that accounts for nonideality of the reference fluid of nonbonded chain segments (monomers), $\tilde{a}^{chain}$ is the chain term that

Table 2. SAFT and SAFT1 Parameters for Polymers and Solvents

	components	m	$(v^{oo})_{bb}$, mL mol^{-1}	$(v^{oo})_{br}$, mL mol^{-1}	$(u^o/k)_{bb}$, K	$(u^o/k)_{br}$, K	$(\lambda)_{bb}$	$(\lambda)_{br}$
SAFT	ethylene	1.464	18.16[a]		212.1[a]		n/a	
	propane	2.696	13.46[a]		193.0[a]		n/a	
	hexene-1	4.508	12.99[a]		204.7[a]		n/a	
	EH-0-120K	4688.7	12.0[a]		210.0[a]		n/a	
	EH-4-80K	2468.3	12.0	12.6	210.0	195.1	n/a	
	EH-15-100K	2235.1	12.0	12.6	210.0	195.1	n/a	
	EH-15-140K	5206.5	12.0	12.6	210.0	195.1	n/a	
SAFT1	ethylene	1.383	14.50		146.8		1.737	
	propane	1.667	16.75		193.2		1.691	
	hexene-1	2.509	21.34		225.6		1.692	
	EH-0-120K	2388.8	25.2		281.9		1.65	
	EH-4-80K	1257.7	25.2	19.6	281.9	210.6	1.65	1.68
	EH-15-100K	1138.9	25.2	19.6	281.9	210.6	1.65	1.68
	EH-15-140K	2652.6	25.2	19.6	281.9	210.6	1.65	1.68

[a] For solvents and polymer without branches, there is only one u^o/k, v^{oo}, and λ for the entire molecule.

accounts for covalent bonding, and $\tilde{a}^{assoc}$ is the association term that accounts for the association such as hydrogen bonding. Since the systems examined in this work do not exhibit specific interactions that can lead to association, we set $\tilde{a}^{assoc}$ equal to zero.

The parameters for both versions of SAFT are the segment number m, the segment molar volume v^{oo} in mL mol^{-1}, and the segment energy u^o/k in K. SAFT1 also requires an extra parameter λ, which is the reduced range of the potential well. All the parameter values used in this work are given in Table 2. The detailed description of the theory and equations are not presented here because they can be found in refs 13 and 14 for SAFT and in ref 15 for SAFT1. These references also provide comparisons between calculated and experimental data for pure components and binary mixtures. Although the polymers used in this work are polydisperse, they are approximated in our SAFT and SAFT1 calculations as monodisperse pseudocomponents.

For small molecules, like ethylene, the pure-component parameters are obtained by fitting experimental vapor pressure and liquid density data. For polymers, like EH, the pure-component parameters are obtained by dividing the polymeric chain into suitable segments and estimating segment parameters. For example, EH is divided into two types of segments, the backbone type and the branch type, as shown in Figure 2, which are connected with three types of bonds: backbone−backbone, backbone−branch, and branch−branch. Each segment type has a unique set of SAFT parameters. The parameters for the backbone-type segments are obtained from a correlation developed for long *n*-alkanes.[13,15,16] For the sake of simplicity, the four carbon side branch are assumed to have the same parameters as *n*-butane. Both SAFT and SAFT1 also require the segment and bond fractions for each polymer. Our previous work describes in detail how to calculate these fractions for ethylene copolymer.[17] Their values for EH are given in Table 3.

In this work, one binary interaction parameter, k_{ij}, is fitted to a small subset of experimental data. Since k_{ij} is found to be temperature dependent, it is correlated versus temperature. The empirical k_{ij} correlations are used for all the other calculations in this work without further readjustment.

Results and Discussion

All the experimental data obtained in this work are given in Tables 4 and 5, and some are plotted in the figures. In all the figures, unless specific legends are given, filled symbols mean the FL pressure, open symbols mean the heating-induced FS temperature, solid curves are calculated from SAFT, and dashed curves are calculated from SAFT1.

Table 3. Bond Fractions and Segment Fractions for Polymers

polymer samples	bb−bb bond fraction[a]	bb−br bond fraction[a]	br−br bond fraction[a]	bb segment fraction	br segment fraction
EH-0-120K	1	0	0	1	0
EH-4-80K	0.929	0.053	0.018	0.929	0.071
EH-15-100K	0.767	0.058	0.175	0.767	0.233
EH-15-140K	0.767	0.058	0.175	0.767	0.233

[a] bb−bb = backbone to backbone, bb−br = backbone to branch, br−br = branch to branch.

Figure 3 shows a plot illustrating the effect of EH concentration on the phase behavior. We find that the EH concentration has a relatively weak effect on the FL pressure and FS temperature in the range of this study. Another way to present the phase behavior is to plot the FL pressure at constant temperature in pressure−concentration coordinates, as shown in Figure 4. The FL pressure curves are found to be flat near the critical polymer concentration, which is characteristic of polymer solutions. The approximate critical polymer concentration is experimentally found to be between 0.05 and 0.15 polymer weight fraction. SAFT and SAFT1 underestimate the critical polymer concentration. This is expected because both SAFT and SAFT1 crudely approximate EH as being monodisperse and hence do not account for the actual differences in polydispersity. In general, the higher the polydispersity index, the greater the critical-point shift toward the higher polymer concentrations;[1] the critical point no longer coincides with the maximum of the cloud-point curve.

One can also plot the FS temperatures at constant pressure in temperature−concentration coordinates, as shown in Figure 5. Both heating- and cooling-induced FS temperatures are reported in Figure 5. In general, as expected, the FS temperature increases with increasing EH concentration. Also, as usual, the heating-induced FS temperatures are systematically higher than those induced by cooling (by about 10 deg). The difference is due to the subcooling effect of the crystal formation during cooling, as is explained earlier. Moreover, the FS temperature increases with increasing pressure.

Table 4. Experimental Data for EH + Propane

polymer (EH weight fraction)	*T*/°C	*P*/bar	transition type[a]
EH-4-80K	180.0	507	FL (DP)
(0.01)	140.0	499	FL (DP)
	100.1	500	FL (DP)
	90.0	503	FL (DP)
	89.5	700	FS*
	91.4	1000	FS*
	95.1	1400	FS*
	78.0	700	FS
	79.4	1000	FS
	82.7	1400	FS
(0.051)	180.0	511	FL (DP)
	140.0	504	FL (DP)
	100.0	504	FL (DP)
	90.0	510	FL (DP)
	91.9	700	FS*
	93.2	1000	FS*
	96.8	1400	FS*
	82.1	700	FS
	83.5	1000	FS
	85.7	1400	FS
(0.148)	180.0	511	FL (BP)
	140.0	504	FL (BP)
	100.1	506	FL (BP)
	98.8	700	FS*
	101.0	1000	FS*
	105.5	1400	FS*
	87.4	700	FS
	89.0	1000	FS
	92.7	1400	FS
EH-15-100K	180.0	446	FL (BP)
(0.15)	140.0	423	FL (BP)
	99.9	397	FL (BP)
	89.9	391	FL (BP)
	70.0	381	FL (BP)
	40.0	373	FL (BP)
EH-15-140K	180.0	429	FL (DP)
(0.009)	140.0	406	FL (DP)
	100.0	379	FL (DP)
	95.1	376	FL (DP)
	80.1	368	FL (DP)
	40.1	390	FL (DP)
(0.152)	180.0	437	FL (BP)
	140.0	415	FL (BP)
	100.0	392	FL (BP)
	80.1	378	FL (BP)

[a] FL(DP) = fluid−liquid (dew point), FL (BP) = fluid−liquid (bubble point), FS* = fluid−solid upon heating, FS = fluid−solid upon cooling.

Figure 6 illustrates the effect of molecular weight on the phase behavior. In general, the FL pressure increases with increasing molecular weight. That is not the case in Figure 6. The FL pressure of EH-15-100K is slightly higher than that of EH-15-140K by about 8 bar. We attribute this to the higher polydispersity (PI) of EH-15-100K, which has a PI of 2.14. Therefore, both SAFT and SAFT1 capture the slope of cloud-point curves but do not account for the polydispersity effect. We also find that the difference in the FL pressures for both EH is insignificant. This is expected when the molecular weight of polymer is large.

To explore how the M_w affects the FL pressure over a boarder M_w range, we simulate with SAFT the FL pressure as a function of EH M_w at constant temperature, BD, and polymer composition, as is shown in Figure 7. The lower the M_w, the greater its effect on the FL pressures.

Figure 8 illustrates the effect of BD on the phase behavior. The FL pressure decreases with increasing BD; increasing BD from 4 to 15, for example, increases the FL pressure by about 70−100 bar. Both SAFT and SAFT1 represent these experimental findings quantitatively. We also simulate with SAFT the FL pressure as a function of the weight percent hexene-1 incorporated in EH, a simple function of BD; an example is plotted in Figure 9.

Figure 8 also reports the experimental FS temperature for EH-4-80K + propane; however, the FS temperature for EH-15-100K is not measured because it is

Table 5. Experimental Data for EH + Ethylene, + Hexene-1, and + Ethylene + Hexene-1

polymer (EH weight fraction) (ethylene weight fraction)[b]	*T*/°C	*P*/bar	transition type[a]
EH-0-120K	182.5	730	FL
(0.147)	172.1	730	FL
(0.49 Eth)	160.3	728	FL
	140.1	742	FL
	125.4	731	FL
	119.7	761	FL
EH-4-80K	180.0	1389	FL (BP)
(0.148)	160.1	1460	FL (BP)
(1.0 Eth)	140.0	1545	FL (BP)
	120.1	1680	FL (BP)
(0.149)	180.2	651	FL (BP)
(0.5 Eth)	150.0	665	FL (BP)
	120.0	654	FL (BP)
	98.1	1000	FS*
	102.6	1400	FS*
	103.6	1550	FS*
	84.3	1000	FS
	84.7	1400	FS
	86.5	1550	FS
(0.139)	180.1	446	FL (BP)
(0.32 Eth)	150.0	451	FL (BP)
	120.1	442	FL (BP)
	101.2	700	FS*
	106.2	1000	FS*
	107.8	1400	FS*
	88.3	700	FS
	91.7	1000	FS
	93.1	1400	FS
(0.150)	101.8	200	FS*
(0.0 Eth)	103.2	500	FS*
	104.8	800	FS*
	89.2	200	FS
	90.9	500	FS
	92.3	800	FS
EH-15-100K	180.0	1210	FL (DP)
(0.05)	170.0	1229	FL (DP)
(1.0 Eth)	160.0	1249	FL (DP)
	150.0	1270	FL (DP)
	140.0	1296	FL (DP)
	130.0	1326	FL (DP)
	120.0	1363	FL (DP)
(0.10)	180.0	1208	FL (BP)
(1.0 Eth)	170.0	1218	FL (BP)
	160.0	1237	FL (BP)
	150.0	1258	FL (BP)
	140.0	1283	FL (BP)
	130.0	1314	FL (BP)
	120.0	1348	FL (BP)
(0.15)	180.0	1194	FL (BP)
(1.0 Eth)	170.0	1187	FL (BP)
	160.0	1198	FL (BP)
	150.0	1215	FL (BP)
	140.0	1236	FL (BP)
	130.0	1261	FL (BP)
	120.0	1294	FL (BP)
(0.14)	180.0	577	FL (BP)
(0.53 Eth)	160.0	562	FL (BP)
	140.0	557	FL (BP)
	120.0	557	FL (BP)

[a] FL (DP) = fluid−liquid (dew point), FL (BP) = fluid−liquid (bubble point), FS* = fluid−solid upon heating, FS = fluid−solid upon cooling. [b] Ethylene weight fraction is in polymer-free basis.

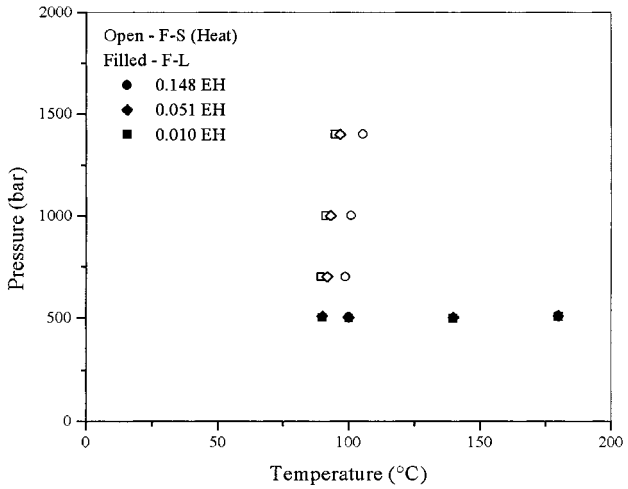

Figure 3. $P-T$ phase diagram for EH-4-80K + propane.

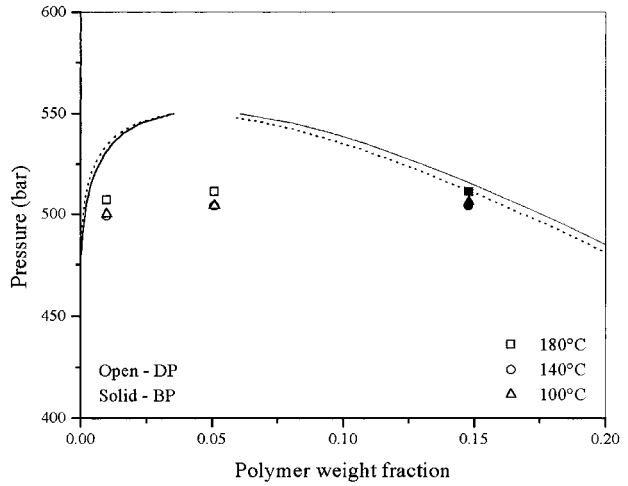

Figure 4. $P-X$ phase diagram for EH-4-80K + propane. Solid line is calculated with SAFT, and dotted line is calculated with SAFT1 at 180 °C.

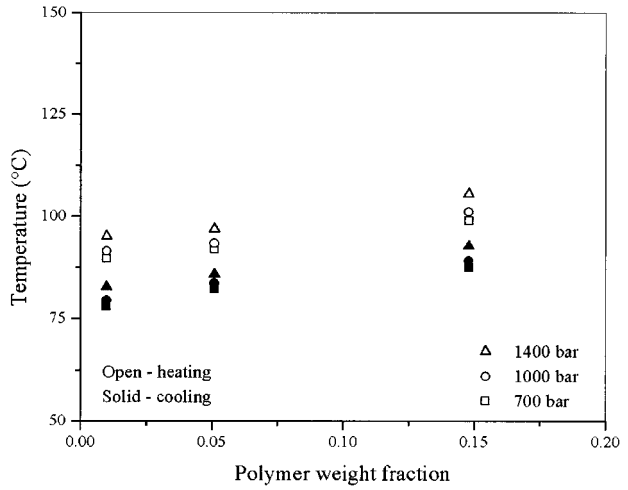

Figure 5. $T-X$ phase diagram for EH-4-80K + propane.

below the room temperature (about 23 °C) in this case. The measured FS temperatures seem to decrease with increasing BD, which is consistent with the trend reported by Chan et al.[17] No attempt is made to calculate the FS temperature with SAFT in this study, because it requires more FS data for polymers with different BD.[17]

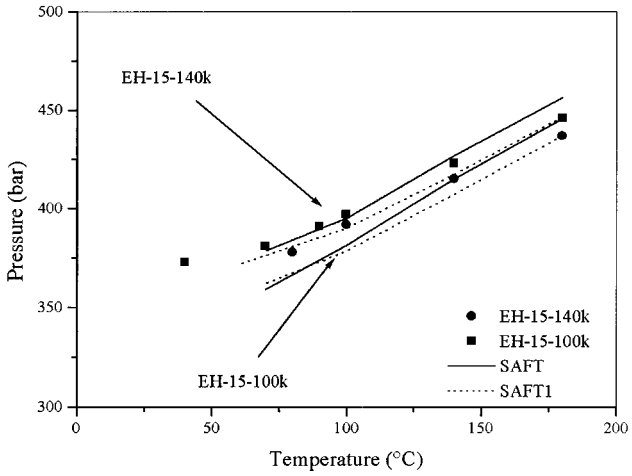

Figure 6. $P-T$ phase diagram for EH-15-100K and EH-15-140K + propane at 0.15 weight fraction polymer.

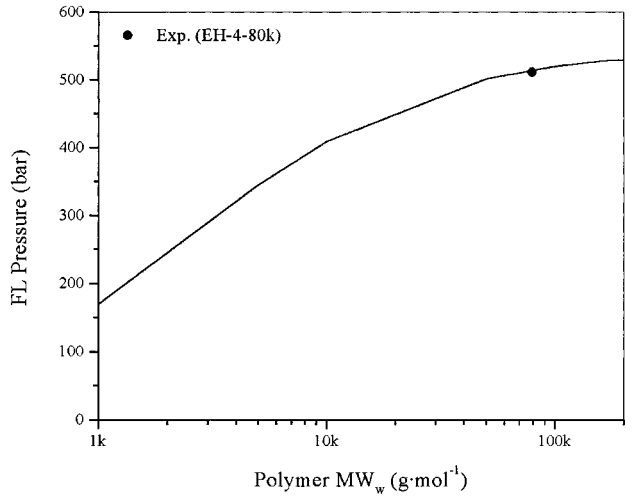

Figure 7. SAFT simulation of molecular weight effect on the FL pressure for EH-4-x + propane at 180 °C.

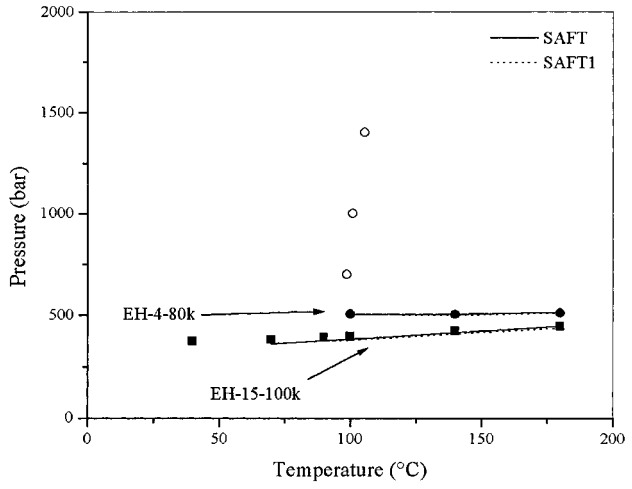

Figure 8. $P-T$ phase diagram for EH-4-80K and EH-15-100K + propane propane at 0.15 weight fraction polymer.

Figure 10 shows the effect of the solvent type on the phase behavior of EH-4-80K and EH-15-100K in ethylene and propane. For example, replacing propane with ethylene as a solvent for EH increases the FL pressure by about 1000 bar, and it causes the LCST-type behavior for propane to become an UCST-type behavior for

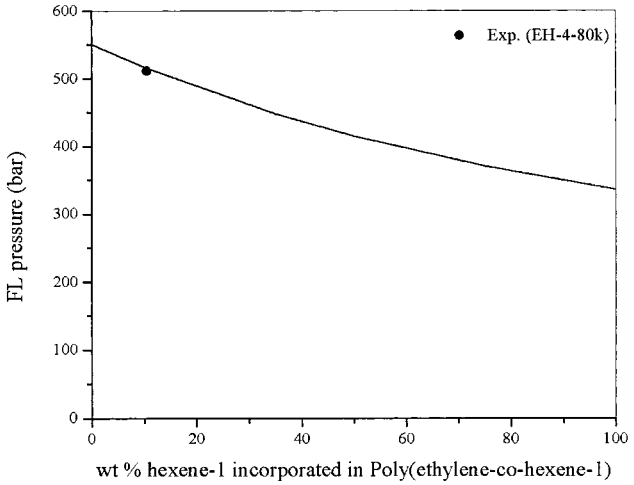

Figure 9. SAFT simulation of BD effect on the FL pressure for EH-*x*-80K + propane at 180 °C.

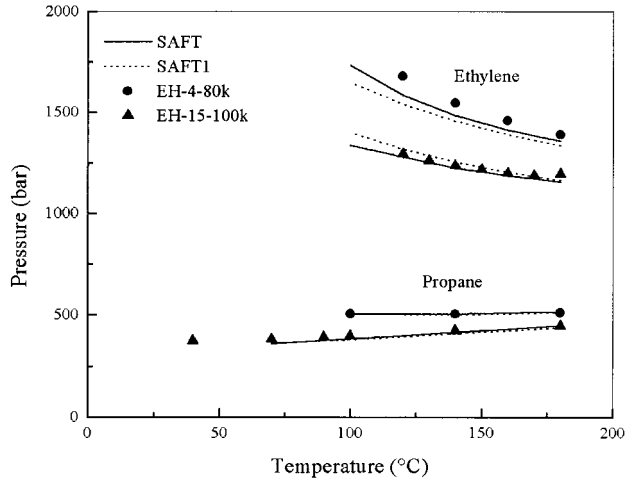

Figure 10. *P*−*T* phase diagram for EH-4-80K and EH-15-140K + propane and + ethylene propane at 0.15 weight fraction polymer.

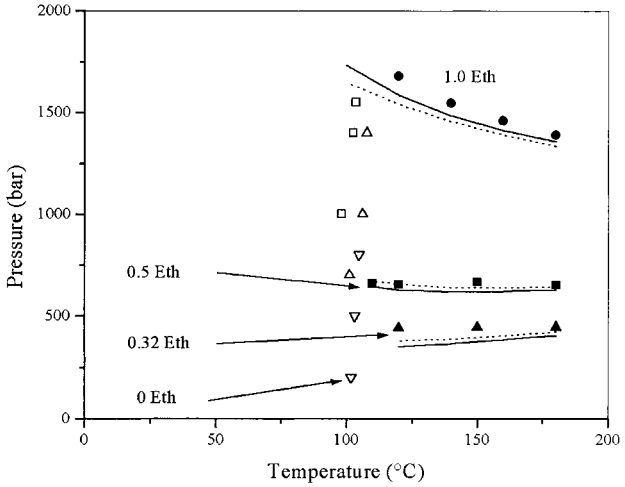

Figure 11. *P*−*T* phase diagram for EH-4-80K + ethylene + hexene-1 propane at 0.15 weight fraction polymer.

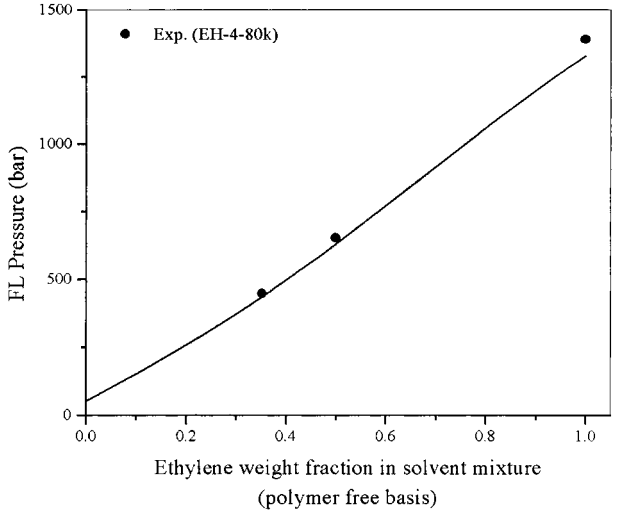

Figure 12. SAFT simulation of solvent ratio effect on the FL pressure and FS temperature for EH-4-80K + ethylene + hexene-1 at 180 °C.

ethylene. This is consistent with the trend induced by the size difference between the polymer and solvent suggested by Folie and Radosz.[1] Also worth noticing in Figure 10 is a large shift in the FL pressure in going from EH-4-80K to EH-15-100K in ethylene, relative to propane; BD seems to have a greater impact on the FL pressure in ethylene.

Figure 11 illustrates the antisolvent effect of ethylene on the FL pressure and FS temperature for EH-4-80K in a series of ethylene + hexene-1 solvents, from pure hexene-1 (0 Eth) to pure ethylene (1 Eth), where the numbers preceding Eth indicate the ethylene weight fraction on a polymer-free basis. Increasing the ethylene concentration in the solvent mixture increases the FL pressure. For example, in going from pure hexene-1 to 0.32 ethylene, the FL pressure increases by about 450 bar. A further addition of ethylene to 0.5 shifts the FL pressure by about 300 bar, and it shifts the FL behavior from LCST to UCST. Both SAFT and SAFT1 quantitatively represent these findings. Since the FL pressure in hexene-1 is too low to measure accurately in this project, we calculate it with SAFT. The results for the whole solvent range are shown in Figure 12. We find that ethylene has a strong antisolvent effect on the FL pressure; for example, increasing the ethylene concentration from 0 to 1.0 increases the FL pressure by nearly 1400 bar.

Increasing the ethylene concentration in the solvent mixture, however, is found to depress the FS temperature by a few degrees. For example, as shown in Figure 11, the FS temperature in pure hexene-1 is 103 °C. An addition of ethylene to 0.5 weight fraction (polymer-free basis) shifts down the FS temperature by about 5 °C. For the record, for pure ethylene, no FS temperature can be observed because it is shifted to temperatures below the FL temperatures, at least in our pressure range (up to about 2000 bar).

To recapitulate, we simulate with SAFT the FL pressure surfaces as a function of weight percent incorporated hexene-1 and another system variable, all at 180 °C. That other system variable is M_w for the EH + propane example shown in Figure 13, and it is ethylene weight fraction in solvent (polymer-free basis) for the EH + ethylene + hexene-1 example shown in Figure 14. The space above each surface is the one-phase space. In Figure 13, a combination of high M_w and low incorporated hexene-1% (low BD) results in the highest FL pressure. The FL surface is relatively flat except in the low molecular weight region, where the

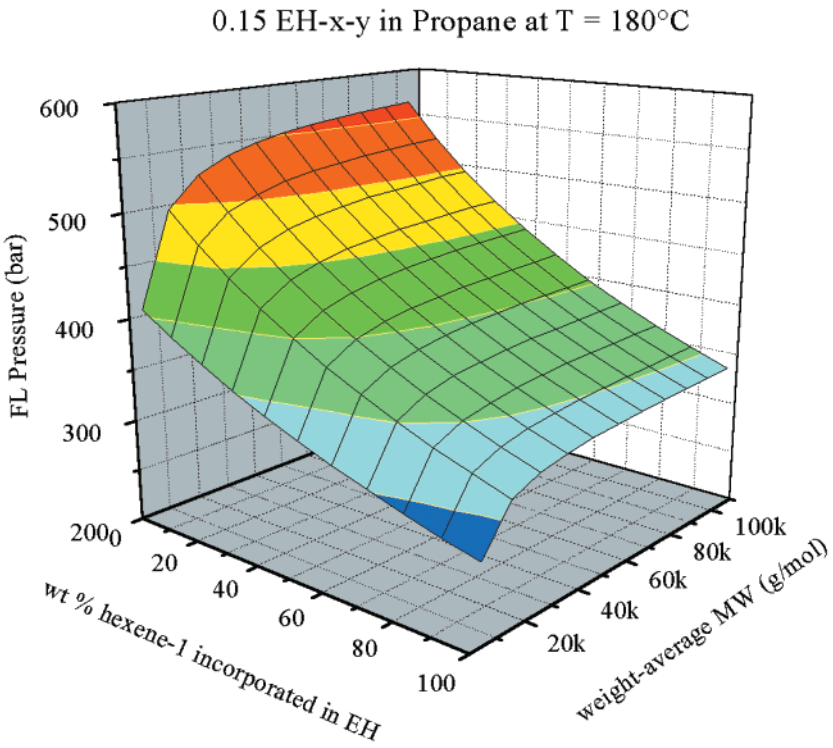

Figure 13. 3D SAFT simulation of wt % hexene-1 incorporated in EH and molecular weight effect on the FL pressure for EH-*x*-*y* + propane at 180 °C.

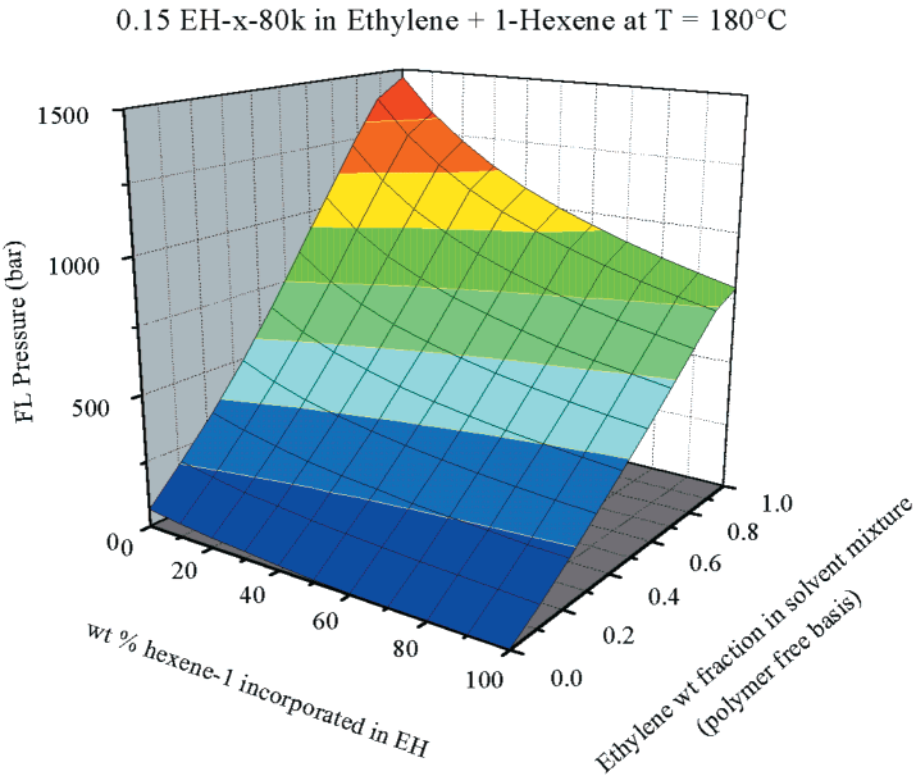

Figure 14. 3D SAFT simulation of wt % hexene-1 incorporated in EH and solvent ratio effect (ethylene weight fraction) on the FL pressure for EH-*x*-*y* in ethylene + hexene-1 at 180 °C.

FL pressure decreases dramatically. In Figure 14, a combination of the high ethylene concentration and low incorporated hexene-1% (low BD) results in the highest FL pressure. The FL surface is much steeper in this case, which illustrates the very high sensitivity of the FL pressure to the ethylene concentration in the solvent mixture.

Conclusions

The effects of the EH concentration, M_w, BD, solvent type, and solvent composition on the FL pressure and FS temperature of EH in propane and, separately, in ethylene + hexene-1 are measured and calculated at temperatures up to 180 °C and at pressures up to 1400 bar. The EH concentration and M_w are found to have a

relatively weak effect. The EH BD has a stronger effect; it tends to decrease both FL pressure and FS temperature. Furthermore, the FL pressure is found to depend strongly on the solvent type and composition; it is found to increase with increasing ethylene concentration. Both SAFT and SAFT1 are found to capture these trends.

References and Notes

(1) Folie, B.; Radosz, M. Phase Equlilibria in High-Pressure Polyethylene Technology. *Ind. Eng. Chem. Res.* **1995**, *34*, 1501.
(2) Charlet, G.; Delmas, G. Thermodynamic Properties of Polyolefin Solutions at High Temperatures: 1. Lower Critical Solubility Temperatures of Polyethylene, Polypropylene and Ethylene-Propylene Copolymers in Hydrocarbon Solvents. *Polymer* **1981**, *22*, 1181−1189.
(3) Chen, S. J.; Radosz, M. Density-Tuned Polyolefin Phase Equilibria. 1. Binary Solutions of Alternating Poly(ethylene-propylene) in Subcritical and Supercritical Propylene, 1-Butene, and 1-Hexene. Experiment and Flory-Patterson Model. *Macromolecules* **1992**, *25*, 3089−3096.
(4) deLoos, T. W.; Poot, W.; Diepen, G. A. M. Fluid Phase Equilibria in the System PE + Ethylene 1. Systems of Linear PE + Ethylene at High Pressure. *Macromolecules* **1983**, *16*, 111−117.
(5) Hasch, B. M.; Lee, S. H.; McHugh, M. A. The Effect of Copolymer Architecture on Solution Behavior. *Fluid Phase Equilib.* **1993**, *83*, 341−348.
(6) Xiong, Y.; Erdogan, K. High-Pressure Phase Behavior in PE/*n*-Butane Binary and PE/*n*-Butane/CO_2 Ternary Systems. *J. Appl. Polym. Sci.* **1994**, *53*, 1179.
(7) Ehrlich, P.; Kurpen, J. J. Phase Equilibria of Polymer−Solvent Systems at High Pressures Near Their Critical Loci: Polyethylene with *n*-Alkanes. *J. Polym. Sci., Part A* **1963**, *1*, 3217−3229.
(8) Ehrlich, P. Phase Equilibria of Polymer−Solvent Systems at High Pressures Near Their Critical Loci. II. Polyethylen-Ethylene. *J. Polym. Sci., Part A* **1965**, *3*, 131−136.
(9) Chan, A. K. C.; Russo, P. S.; Radosz, M. Fluid-Liquid Equilibria in Poly(ethylene-*co*-hexene-1) + Propane: A Light-Scattering Probe of Cloud-Point Pressure and Critical Polymer Concentration. *Fluid Phase Equilib.* **2000**, *4450*, 1−10.
(10) Kohn, J. P.; Luks, K. D.; Liu, P. H. Three-Phase Solid−Liquid-Vapor Equilibria of Binary-*n*-Alkane Systems (Ethane-*n*-Octane, Ethane-*n*-Decane, Ethane-*n*-Dodecane). *J. Chem. Eng. Data* **1976**, *21*, 360−362.
(11) Condo, P. D.; Colman, E. J.; Ehrlich, P. Phase Equilibria of Linear Polyethylene with Supercritical Propane. *Macromolecules* **1992**, *25*, 750.
(12) Spahl, R.; Luft, G. Entmischungsverhalten von Ethylen und niedermolekularem Polyethylen. *Ber. Bunsen-Ges. Phys. Chem.* **1981**, *85*, 379−384.
(13) Huang, S. H.; Radosz, M. Equation of State for Small, Large, Polydisperse, and Associating Molecules. *Ind. Eng. Chem. Res.* **1990**, *29*, 2284−2294.
(14) Banaszak, M.; Chen, C. K.; Radosz, M. Copolymer SAFT Equation of State. Thermodynamic Perturbation Theory Extended to Heterobonded Chains. *Macromolecules* **1996**, *29*, 6481−6486.
(15) Adidharma, H.; Radosz, M. Prototype of an Engineering Equation of State for Heterosegmented Polymers. *Ind. Eng. Chem. Res.* **1998**, *37*, 4453−4462.
(16) Huang, S. H.; Radosz, M. Equation of State for Small, Large, Polydisperse, and Associating Molecules: Extension to Fluid Mixtures. *Ind. Eng. Chem. Res.* **1991**, *30*, 1994−2005.
(17) Chan, A. K. C.; Adidharma, H.; Radosz, M. Fluid-Liquid and Fluid-Solid Transitions of Poly(ethylene-*co*-octene-1) in Sub- and Supercritical Propane Solutions. *Ind. Eng. Chem. Res.*, in press.
(18) Chan, A. K. C.; Adidharma, H.; Radosz, M. Fluid-Liquid Transitions of Poly(ethylene-*co*-octene-1) in Supercritical Ethylene Solutions. *Ind. Eng. Chem. Res.*, in press.

MA991994K